Model of Temperature Dependence for Gain Shape of Erbium-Doped Fiber Amplifier

Maxim Bolshtyansky, Paul Wysocki, and Nicholas Conti

***Abstract*—The problem of modeling the temperature dependence of erbium-doped fiber amplifier (EDFAs) is important for multichannel optical WDM systems. A physical model is presented in this paper, which could be used to predict the gain change under temperature variations for such systems. Some of the input parameters for the model are the erbium energy sublevel density, excitation coefficients from lower sublevels to upper sublevels of erbium ions, and electron distribution over energy levels. It is difficult to measure these parameters. In order to use the model for gain shape calculations, some simplifications are demonstrated. These simplifications lead to two numerical models, which are shown to be consistent with experimental data with reasonable accuracy, and are based only on two spectral measurements for different temperatures. Both numerical models were tested for the signal band and the 980 nm pump band of a typical erbium-doped fiber.**

***Index Terms*—McCumber's relation, optical fiber amplification, optical fiber thermal factors.**

I. Introduction

In a typical WDM system, most components exhibit some temperature dependence in loss shape and/or magnitude. Early systems often had enough margin in performance that such changes could be tolerated. However, as systems evolve toward more wavelengths, higher bit rates and greater distances, such temperature dependencies are no longer acceptable. Rare-earth ions such as erbium in a silica host are generally considered to be insensitive to temperature. However, in a typical erbium-doped fiber amplifier (EDFA), the erbium provides between 15 and 45 dB of gain. The erbium fiber gain compensates for the losses of components placed within the EDFA and also provides the net gain of the amplifier. A 1% change in the gain coefficient of the EDF with temperature translates to a 0.3 dB gain difference in a typical EDFA with 30 dB of erbium gain. This change is a significant part of the available margin in an EDFA required to achieve flatness within 1 dB. Hence, the temperature dependence of the erbium ions is an important part of the overall temperature dependence of an EDFA. While several authors have recognized the presence and significance of this dependence [1]–[4], no general rule for predicting the temperature dependence of a particular EDFA has been presented.

Linear extrapolation techniques have been used by several authors [3], [4] to model the temperature dependence of EDFAs. While this approach can be used for a small temperature variation, a better approach is needed in order to achieve a good accuracy for a wide temperature range. Such an approach based on the physical model will be developed below.

Manuscript received May 18, 2000; revised August 9, 2000. This work was done while the authors were with Lucent Technologies.

M. Bolshtyansky and P. Wysocki are with Onetta, Bridgewater, NJ 08807 USA (e-mail: maxim@onetta.com).

N. Conti is with Lucent Technologies, Somerset, NJ 08873 USA.

Publisher Item Identifier S 0733-8724(00)09825-X.

II. Theoretical Model

Before going into a description of the energy levels of an erbium ion in a glass host, consider first a simple system with discrete levels. The levels of this system can be degenerate. Let N be the concentration of active ions in the media and n_i be the probability of electron to be at level i. By definition of probability

$$\sum_i n_i = 1. \tag{1}$$

If a plane wave with frequency ν and intensity I propagates along the z-axis through the medium, its evolution can be described by, see, for example, [5]

$$I(z) = I_0 e^{g \cdot z} \tag{2}$$

where g is the gain coefficient defined by

$$g = \sigma_{ul} N \left[n_u - \frac{w_u}{w_l} n_l \right]. \tag{3}$$

Here σ_{ul} is the stimulated emission cross section, w_i is the statistical weight of the ith level, and the electron transition occurs between the upper level with $i = u$ and the lower level with $i = l$, separated by an energy difference $E_{ul} = h\nu$.

If several energy levels are separated by equal distance $h\nu$, then a summation over all such levels is required

$$g(\nu) = \sum_{E_i - E_j = h\nu} \sigma_{ij} N \left[n_i - \frac{w_i}{w_j} n_j \right]. \tag{4}$$

The initial and terminal energy manifolds that produce gain in an EDFA consist of seven and eight broadened levels, respectively. Each level can be further divided into vibration sublevels. In this paper we use a continuous level density approximation to describe each erbium ion manifold. The shape of the level density is not expected to be a function of temperature. Hence, the temperature dependence of an EDF is mainly due to the variation in the occupation probability density within each manifold. In particular, the relative occupation of two levels in thermal equilibrium follows Boltzmann's law:

$$\frac{P(E_2)}{P(E_1)} = e^{-[E_2 - E_1/kT]} \tag{5}$$

where T is the temperature in degrees Kelvin and k is Boltzmann's constant. The most general form of the function $P(E)$

which satisfies condition (5) is

$$P(E) = \exp\left(-\frac{E}{kT}\right) \cdot f(T). \tag{6}$$

Here $f(T)$ is an arbitrary function of temperature, which will be defined later by satisfying a normalization condition. Because each manifold is of finite extent, we can apply the same fundamental principal as for (1) that the sum of all occupation probabilities for all states of the manifold must equal one (assuming the ion is excited to manifold m). Using that rule and defining the lowest and highest energy levels in the manifold m as E_m^L and E_m^{H}

$$\int_{E_m^L}^{E_m^H} \rho(E) P_m(E)\, dE = f_m(T) \int_{E_m^L}^{E_m^H} \rho(E) \exp\left(-\frac{E}{kT}\right) dE = 1 \tag{7}$$

where $\rho(E)$ is the energy density of states. This equation should be satisfied for all temperatures T and is equivalent to equation (1) for the continuous level density case. Function $f_m(T)$ is defined by this equation.

Suppose that there are two identical manifold u and l, that is $\rho(E) = \rho(E - \Delta E)$ for some energy range, and ΔE is the distance between those manifolds. Then condition (7) can be satisfied if

$$P_u(E) = \exp\left(-\frac{E - \Delta E}{kT}\right) \cdot f_u(T) \tag{8}$$

$$P_l(E) = \exp\left(-\frac{E}{kT}\right) \cdot f_l(T) \tag{9}$$

and

$$f_u(T) = f_l(T). \tag{10}$$

Of course, the erbium ion level density is different for different manifolds and, as a result, (10) is not valid; but, we still would like to use (8) and (9) for definitions of P_u and P_l. This is especially valuable in the case that the level densities for the upper and lower manifolds are not very different, and functions f_u and f_l are similar.

Equation (4) can be transformed for a continuous erbium ion spectrum by changing the summation into an integration over E, substituting $\rho(E)P(E)$ for n_i and substituting $\rho(E+h\nu)/\rho(E)$ for w_i/w_j:

$$g(\nu) = \int_0^\infty \sigma(E + h\nu, E) N \left[\rho(E + h\nu) P(E + h\nu) - \frac{\rho(E + h\nu)}{\rho(E)} \rho(E) P(E)\right] dE. \tag{11}$$

When only the upper manifold is occupied, the equation yields

$$g(\nu) = g^*(\nu) = N \int_0^\infty \sigma(E + h\nu, E) \rho(E + h\nu) P_u(E + h\nu)\, dE. \tag{12}$$

For occupied low manifold, (11) gives

$$g(\nu) = -\alpha = -N \int_0^\infty \sigma(E + h\nu, E) \rho(E + h\nu) P_l(E)\, dE. \tag{13}$$

Here P_u and P_l stand for distributions for upper and lower manifold occupied, respectively. Substitution of (8) and (9) into (12) and (13) gives expression for absorption and emission coefficients α and g^*

$$\alpha(\nu) = N \cdot f_l(T) \cdot \int_0^\infty \sigma(E + h\nu, E) \rho(E + h\nu) \cdot \exp\left(-\frac{E}{kT}\right) dE \tag{14}$$

$$g^*(\nu) = N \cdot f_u(T) \cdot \exp\left(\frac{\Delta E - h\nu}{kT}\right) \cdot \int_0^\infty \sigma(E + h\nu, E) \rho(E + h\nu) \exp\left(-\frac{E}{kT}\right) dE. \tag{15}$$

This set of equations is the basis of our numerical model and will be discussed later. Knowledge of the temperature dependence of g^* and α is very important for calculation of amplifier performance, because the gain of an erbium-doped fiber can be expressed via these parameters [6]

$$g(\nu, Inv) = \frac{1}{P(\nu)} \frac{dP(\nu)}{dz} = [g^*(\nu) + \alpha(\nu)] Inv - \alpha(\nu) - L(\nu) \tag{16}$$

where $L(\nu)$ is the background loss of the fiber and Inv is the local inversion of the erbium ions (fraction of ions in the first excited state).

Comparison of (14) and (15) gives

$$g^*(\nu) = \alpha(\nu) \cdot \frac{f_u(T)}{f_l(T)} \cdot \exp\left(\frac{\Delta E - h\nu}{kT}\right). \tag{17}$$

This expression can be rewritten as

$$g^*(\nu) = \alpha(\nu) \cdot \exp\left(\frac{\Delta E'(T) - h\nu}{kT}\right) \tag{18}$$

$$\Delta E'(T) = \Delta E + \ln\left(\frac{f_u(T)}{f_l(T)}\right). \tag{19}$$

Because of logarithmic dependence in (19), $\Delta E'(T)$ could be considered constant for moderate change in temperature. Moreover for similar manifold structure $\Delta E'$ is close to ΔE. Equation (18) is known in the literature as McCumber's relation [7]–[9], though it was derived here using a different method and assumptions. This relation has been checked experimentally in the range from –40°C up to 80°C. The experimental measurements were unable to find any temperature dependence of $\Delta E'$ on T.

It should be mentioned here that the derivations above were done under the assumption that all Er ions are identical, that is that they have identical energy level density $\rho(E)$ and stimulated emission cross section σ. In reality this is not completely true, because each Er ion can have a slightly different neighbor-

hood and thus all equations should be averaged over different ions. However experimental results show that this is a small correction and one can still use McCumber's relation (18). As we will show later, the numerical model based on (15) also gives good accuracy.

III. Numerical Models

In this section we will primary discuss how to use equation (14) for "real life" calculations. The general procedure is to first calculate α for a given temperature using (14), then to find g^* using McCumber's relation (18), and finally to obtain gain g using (16) for a known inversion and background loss. However, functions that are needed for absorption calculation include f_l, the cross section σ, and the level density ρ. These are very hard or impossible to measure or calculate. Hence big simplifications are needed in order to use the formula.

A first simplification is in the calculation of f_l. We suggest assuming that in the normalization condition (7) the level density $\rho(E)$ is constant for $E > E_l^L$ and zero otherwise. We use here notation E_l instead of E_m to show that we deal with the lower manifold. Because the results of the computation should not depend on the location of the energy reference level, one can put $E_l^L = 0$. Taking the limit of $E_l^H \to \infty$ one can find that

$$f_l(T) = \frac{c}{T} \tag{20}$$

where c is some constant. A second suggestion is to substitute integration in (14) by a finite summation. Moreover, because of the relatively short temperature range of interest (about 100 °C) we would like to keep only two terms in that sum! Thus the whole expression can be replaced by a very simple sum

$$\alpha(\lambda, T) = \frac{1}{T}\left(F_1(\lambda)\cdot e^{-E_1/kT} + F_2(\lambda)\cdot e^{-E_2/kT}\right) \tag{21}$$

where $F_1(\lambda)$ and $F_2(\lambda)$ are some functions of wavelength λ, but not of temperature T. They are related somehow to cross section σ and level density ρ, but this relation is not important now because we define those functions from actual measurements.

Given two different spectra $\alpha_a(\lambda)$ and $\alpha_b(\lambda)$ at two different temperatures T_a and T_b, one can derive the following system of equations from (21):

$$\begin{pmatrix}\alpha_a(\nu)\\ \alpha_b(\nu)\end{pmatrix} = C\cdot\begin{pmatrix}F_1(l)\\ F_2(l)\end{pmatrix}$$
$$C = \begin{pmatrix}\frac{1}{T_a}e^{-T_1/T_a} & \frac{1}{T_a}e^{-T_2/T_a}\\ \frac{1}{T_b}e^{-T_1/T_b} & \frac{1}{T_b}e^{-T_2/T_b}\end{pmatrix} \tag{22}$$

where $T_i = E_i/k$. Thus, $F_1(l)$ and $F_2(l)$ can be easily calculated

$$\begin{pmatrix}F_1(l)\\ F_2(l)\end{pmatrix} = C^{-1}\cdot\begin{pmatrix}\alpha_a(\nu)\\ \alpha_b(\nu)\end{pmatrix} \tag{23}$$

and then they can be used in (21) for spectrum evaluation for various temperatures. In addition to $F_1(\lambda)$ and $F_2(\lambda)$, which are already found, (21) contains two parameters T_1 and T_2, which should be defined. Intuitively, one should take T_1 and T_2 above and below the temperature region of interest. We made a numerical optimization of these parameters in order to best-fit experimental dependencies. The optimum T_1 and T_2 are to be found 90K and 650K.

It is interesting to note that for the long wavelength part of the spectrum, the second (high temperature) term in (21) dominates. This means that we can neglect the first term for this region. In fact, we can even suggest dropping the preexponential multiplier to get a different kind of approximation

$$\alpha(\lambda, T) = \alpha(\lambda, \infty)e^{[\beta_a(\lambda)/kT]} \tag{24}$$

where $\alpha(\lambda, \infty)$ and $\beta_a(\lambda)$ are some functions to be defined from two spectra at different temperatures. The fact that we used the function $\beta_a(\lambda)/k$ instead of just the constant T_2 helps to improve the precision for a wider wavelength range and compensates for neglecting the first term in equation (21) and for dropping the $1/T$ preexponential multiplier. A similar formula can be used for a g^* approximation

$$g^*(\lambda, T) = g^*(\lambda, \infty)e^{[\beta_e(\lambda)/kT]}. \tag{25}$$

The fitting parameters $\alpha(\lambda, \infty)$ and $g^*(\lambda, \infty)$ are both temperature independent and can be interpreted as the absorption and gain at infinite temperature when all energy levels of each manifold are equally occupied. The parameters $\beta_a(\lambda)$ and $\beta_e(\lambda)$ are expected to capture the thermal occupation probability of the initial energy level for the transition at a given wavelength. Moreover, if McCumber's relation (18) holds and $\Delta E'$ does not depend on temperature, then

$$\alpha(\lambda, \infty) = g^*(\lambda, \infty) \tag{26}$$

$$\beta_a(\lambda) = \beta_e(\lambda) + \Delta E' - hc/\lambda. \tag{27}$$

Even though the simplified model described by (24) is not as good as the model described by (21) for the short wavelength range, it has its own advantages. First of all, it is simpler, and it does not need two additional parameters T_1 and T_2. Second, it is easier to use this model for different erbium doped fibers, when only one spectrum is known for a certain temperature. Namely, for different fiber, one can correct $\alpha(\lambda, \infty)$ in such a way that (24) gives correct spectrum at that temperature for the same $\beta_a(\lambda)$ as for our initial fiber. In this way spectra at other temperatures can be estimated. Spectral dependencies of g^* can be estimated by a similar technique.

IV. Fitting Results

In order to compare the technique with experimental data, we used a typical high aluminum (12 M% Al) silica-based EDF. The absorption and emission spectra were measured via cutback method at temperatures −40, −20, 0, 20, 40, 60, 80°C for both signal band (1450–1650 nm) and pump band (900–1050 nm). The spectra at −40 °C and at 80 °C were used as input spectra for (23). The experimental and fitting spectra of absorption for the signal band are shown in Fig. 1. Only spectra at −40, 0, 40, and 80 °C are shown for better clarity. The experimental curves are solid and fit curves are dotted. The fit is so good that it is practically not possible to see the difference between the

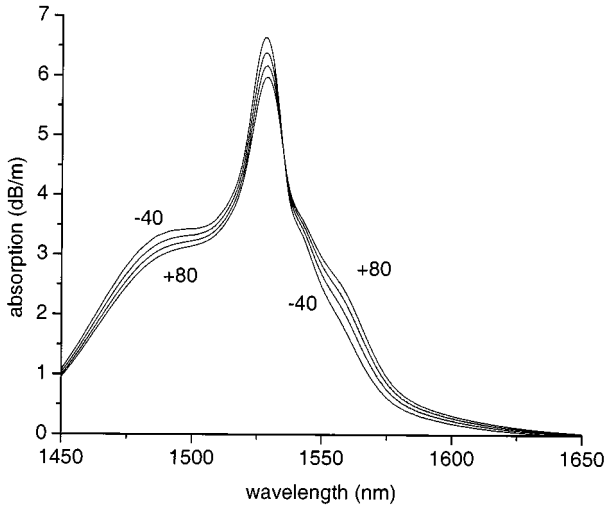

Fig. 1. Measured absorption spectrums (solid lines) and fitting spectrums (dotted lines) at temperatures −40, 0, 40, and 80 °C.

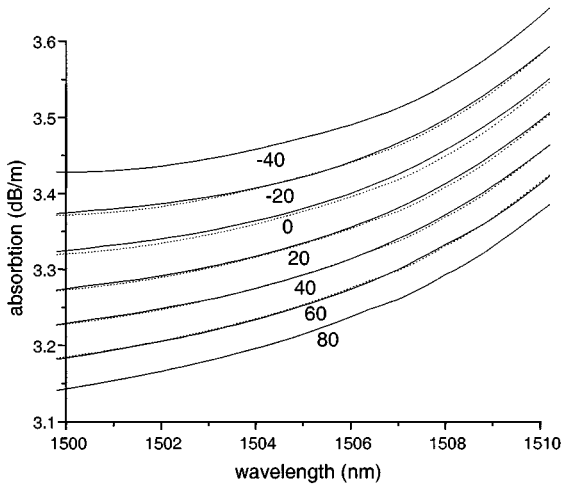

Fig. 2. Part of absorption spectrums (solid lines) and fitting spectrums (dotted lines) from the Fig. 1 under grater magnifications. New measured and fitting spectrums at temperature −20, 20, and 60 °C are added. Numbers near spectrums shows temperatures of the fiber at which spectrums were taken.

fit and the measured data. Fig. 2 shows part of the spectrums of the Fig. 1 under greater magnification. In this figure all seven spectra are shown. You can see that fit is really good, and it is within experimental measurement error. The spectrum fit at −40 and 80 °C is perfect because these spectrums were used in (23).

Fig. 3 shows the functions $F_1(\lambda)$ and $F_2(\lambda)$ used for the fitting of Fig. 1. Simple physical interpretation is possible for those functions. Since (21) is a substitution for (14), F_1 can be treated as the absorption provided by the low temperature portion of the electron distribution within the erbium ground-state manifold, and F_2 can represent the high temperature portion. Both $F_1(\lambda)$ and $F_2(\lambda)$ are found to be positive functions, and their behavior is reasonable for low-temperature and high-temperature excited electrons.

As we have mentioned before, the simplified approximation (24) works well for the long wavelength region of the spectrum but is not as precise as (21) for wavelengths shorter than 1540 nm. To demonstrate this we show in Fig. 4 the same region as for Fig. 2, with the fit using the simplified approximation (21). Again the approximation guaranteed that the spectra at −40 and at 80 °C were exactly fit. The use of different fitting functions for $\alpha(\lambda, \infty)$ and $\beta_a(\lambda)$ can improve the accuracy of the simplified approach if we are interesting only in a −40–60 °C temperature range. Fig. 4(b) shows the simplified fit when the −20 °C and 40 °C spectra were used for $\alpha(\lambda, \infty)$ and $\beta_a(\lambda)$ calculation instead of −40 °C and 80°C pair. You can see much better fit now.

Fig. 5 shows the measured gain coefficient for the same fiber over several temperatures. For simplicity of display only the end temperatures are labeled in Fig. 5. Again, only spectra at −40, 0, 40, and 80 °C are shown for better clarity. The gain coefficients of Fig. 5 represent the gain measured for a short section of EDF pumped by over 300 mW at 980 nm, as interpreted from the resultant ASE spectra measured. As such, they show the existence of signal-band ESA above 1600 nm and also include losses produced by fiber scattering and uninverted erbium ions. The simplified fit is reasonably good over this temperature range. The greatest errors occur at the short and long wavelengths in the

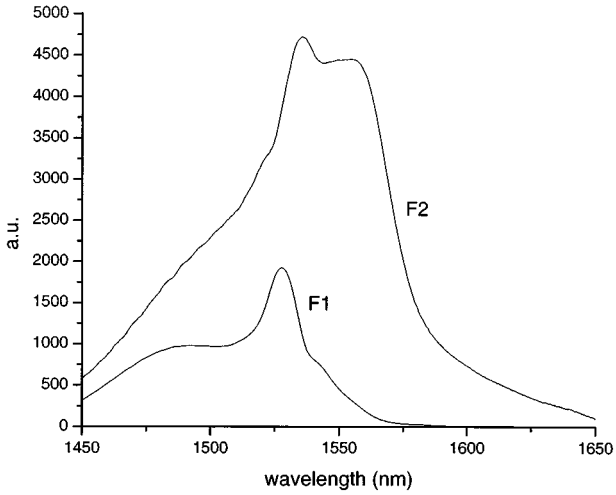

Fig. 3. Functions F_1 and F_2 used for fitting procedure.

gain parameter plots. The small value of gain in these wavelength ranges makes measurements difficult over temperature. At short wavelengths, complete inversion is critical for a good measurement and may not have been achieved in these measurements. At long wavelengths, the presence of signal band ESA is a complication.

The exponential fitting parameters used are shown in Fig. 6. The dashed line is the exponential coefficient $\beta_a(\lambda)/k$ for the absorption while the dotted line is the exponential coefficient $\beta_e(\lambda)/k$ for the gain. We would like to stress that these coefficients were obtained from independent experimental measurements of emission and absorption spectra at different temperatures, and were used in fitting procedure in Figs. 4(b) and 5. The solid line in Fig. 6 shows the exponential coefficient $\beta_e(\lambda)$, which was calculated using formula (27). The good overlap of the solid and dotted lines shows the validity of McCumber relation (18) and the absence of temperature dependence of E' in (18) and (19). In fact, the greatest in accuracy is believed to be in the gain measurements that generated the dotted curve. The

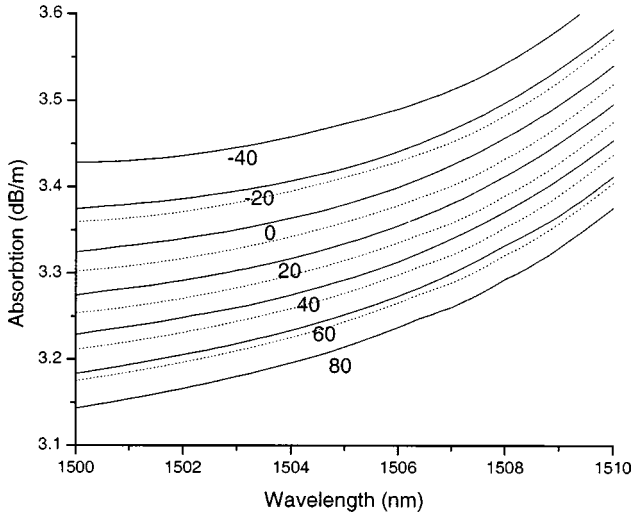

(a)

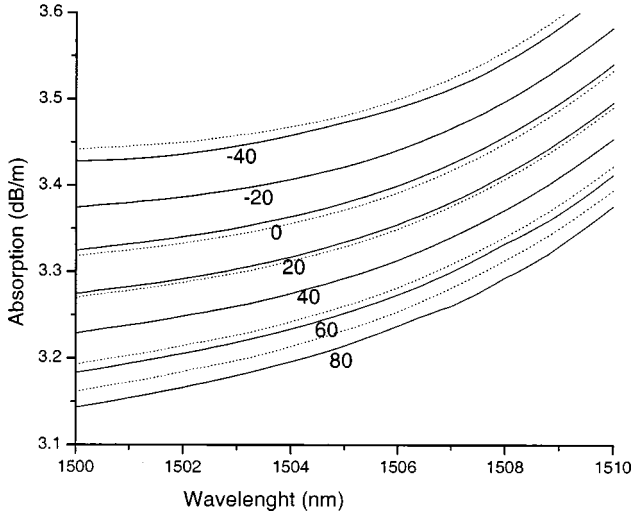

(b)

Fig. 4. Two examples of simplified fit. Solid lines are measured absorption spectrums, dotted lines are fitting spectrums. (a) Absorption spectrums measured at −40 and 80 °C were used for fitting parameters calculation; (b) Absorption spectrums measured at −20 and 40°C were used for fitting parameters calculation.

fact that this curve is not smooth points to measurement error and not to an error in the theory.

Fig. 7 shows fitting parameter plots $\alpha(\lambda, \infty)$ and $g^*(\lambda, \infty)$. Again, according to (26), which is a result of McCumber relation (18), the plots are overlapping with very good accuracy. These plots both represent the summation of all transitions (either upward or downward) when all sublevels of the manifold involved are equally occupied. Hence, this plot shows the relative strengths of the transitions participating at each wavelength when the temperature dependence of the level occupation is removed.

Both the original model of (21) and the simplified model of (25) show much better precision in comparison with the linear fit suggested in [3], [4]. For example, at 1550 nm the model error for 20 °C spectra was 0.25% for the original model, 0.34% for the simplified model, and 1.7% for a linear fit. Again, the same pair of spectra (at −40 and 80 °C) were used in order to calculate

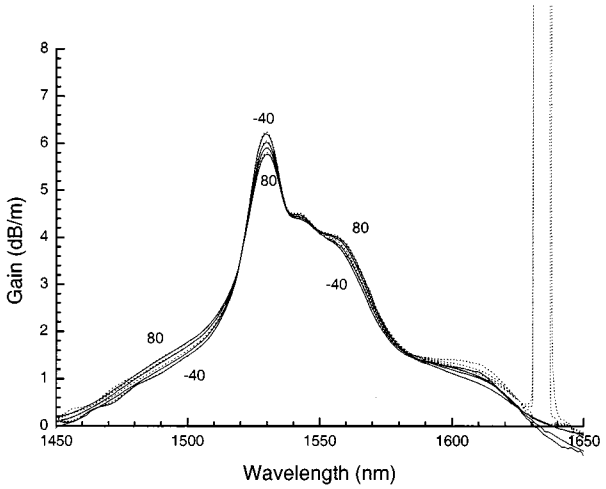

Fig. 5. Measured emission spectrums (solid lines) and simplified fitting spectrums (dotted lines) at temperatures −40, 0, 40, and 80 °C.

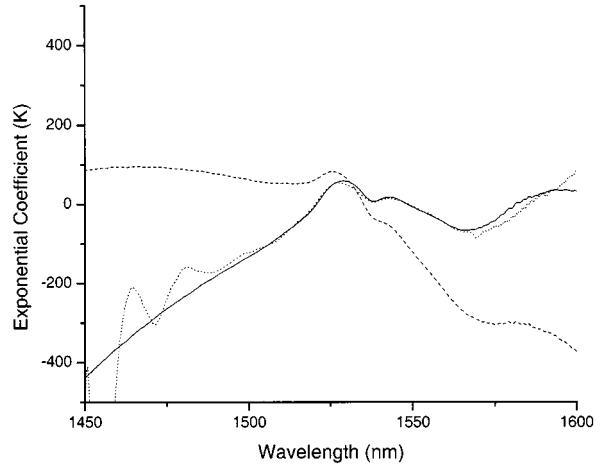

Fig. 6. Fit function $\beta_a(\lambda)/k$, dashed line; and two versions of fit function $\beta_e(\lambda)/k$, solid and dotted lines.

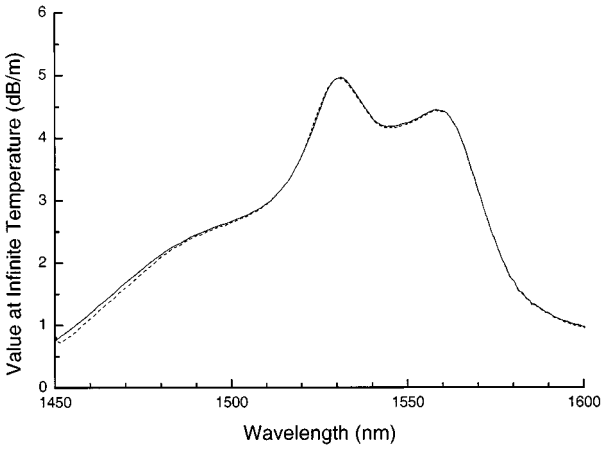

Fig. 7. Fit functions $\alpha(\lambda, \infty)$, dotted line, and $g^*(\lambda, \infty)$, solid line.

fitting parameters for all models. As one can see, the error of the linear fit is an order of magnitude higher than the error of other models described here. This difference is expected to be even more dramatic for wider temperature ranges. As it was mentioned before, a simplified model gives excellent accuracy for

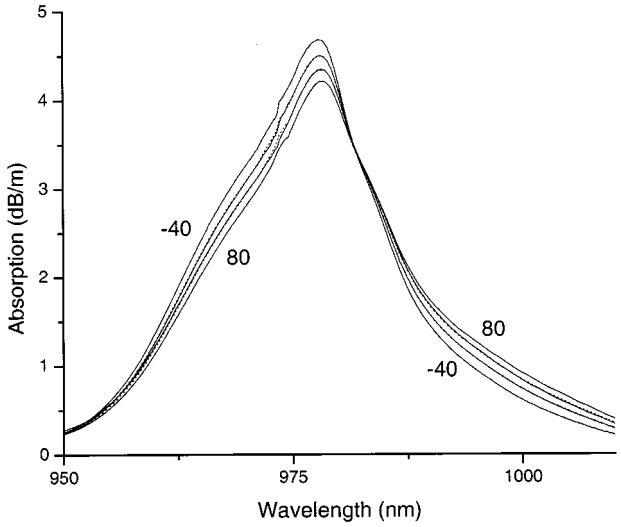

Fig. 8. Measured absorption spectrums (solid lines) and fitting spectrums (dotted lines) for erbium pump band at temperatures −40, 0, 40, and 80 °C.

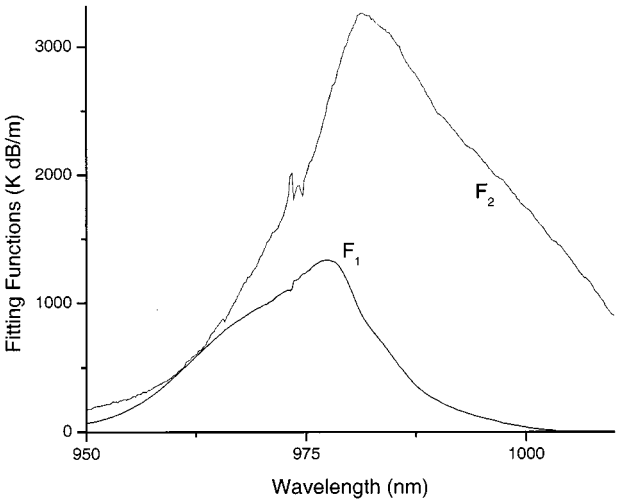

Fig. 9. Functions F_1 and F_2 used for fitting procedure for erbium pump band.

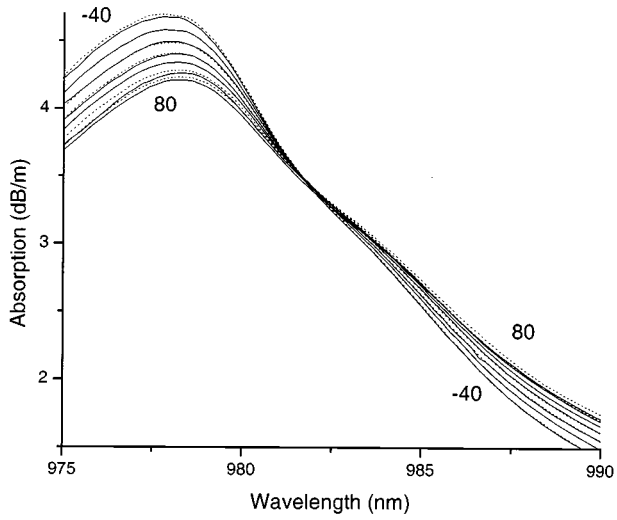

Fig. 10. Part of the measured absorption spectrums (solid lines) and simplified fitting spectrums (dotted lines) for erbium pump band at temperatures −40 , −20, 0, 20, 40, 60, and 80°C.

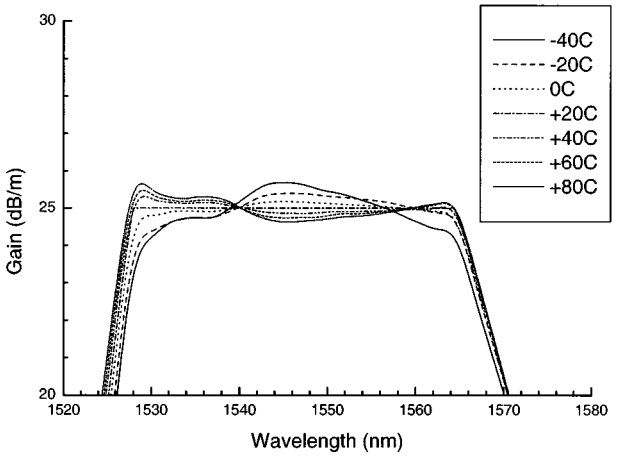

Fig. 11. Predicted gain shape dependence of an EDFA on temperature. EDFA is ideally filtered to 25 dB flat gain from 1528–1563 nm at $T = 20$C. EDFA operates in constant average gain mode (pump adjusts to keep average gain across spectrum constant).

wavelengths larger than 1540 nm, and only the original model of (21) can be used in order to achieve the best precision for the other wavelengths.

To complete the picture of the temperature dependence of an EDF, the temperature dependence of the ground-state absorption near 980 nm has been measured. The data measured by a standard cutback technique for the fiber treated here is shown in Fig. 8 (solid lines). The 980 nm pump band parameters are noisier than those measured in the 1550 nm band because a much weaker white light source was used for the 980 nm measurements. The errors seen below 950 nm are present because the fiber cutoff wavelength is just below 950 nm, which lead to excitation of nonfundamental modes in the fiber. In most of the wavelength range typically used for EDFA pumping, the pump absorption drops as the temperature is increased. Operation at high temperatures is therefore expected to produce a penalty in noise figure for many EDFA designs.

The dotted lines in Fig. 8 represent the fit using (21). The fit is excellent for this data. As in case of the signal band, the measured absorption spectra at −40 °C and 80 °C were input parameters for equation (23). Obtained functions $F_1(\lambda)$ and $F_2(\lambda)$ are shown in Fig. 9. A simplified fit in the form of equation (24) also works well here, although as in the signal band, the long wavelength band is fit better than the short wavelength band. Fig. 10 illustrates this statement by showing part of the fitting curves under greater magnification. Still, the fit is pretty good.

The same logic that was applied above to generate the fitting form of either (21) or (24) should also apply to other rare-earth ions. The authors have checked this by measuring and fitting the absorption of Ytterbium in the 800–1200 nm range. The fit, not shown here, is excellent across the entire band. The gain parameter of Yb was not fit because it is much more difficult to measure precisely than the erbium gain coefficient. It is possible that in other rare-earths, the fit might not be as good. This might especially be true of more inhomogeneously broadened ions such as Neodymium. In this case, equation (24) might apply for subsets of ions but not across all ions, and more terms might be needed in (21). This is an interested area of further research.

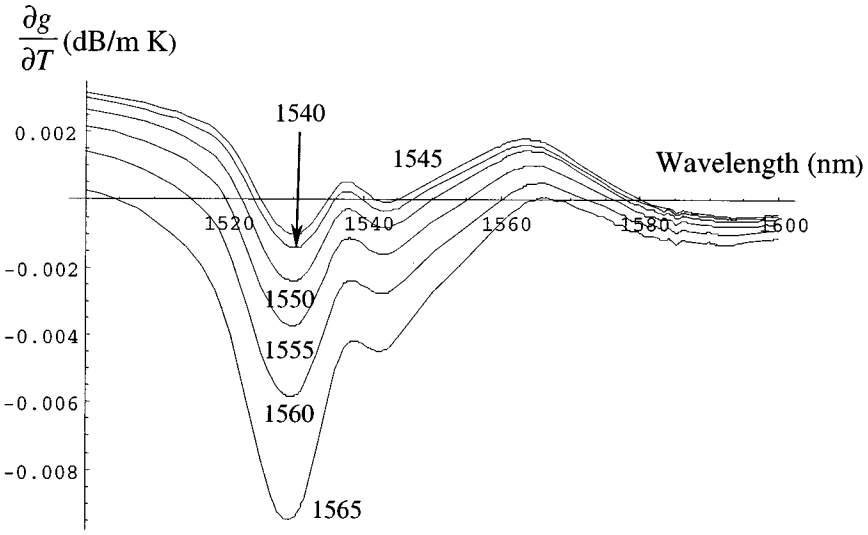

Fig. 12. $\partial g/\partial T$ for fixed $g = 3$ dB/m at different wavelengths. The wavelength numbers are shown near correspondent plots.

V. The Use of the Models

The excellent fit observed to the form of (21) or (24) simplifies computer modeling of temperature dependent gain in an EDFA. A single room temperature measurement of the gain and absorption coefficients of an EDF, combined with the fitting coefficients, is all that is required. From this data, accurate gain and absorption coefficients can be derived at any temperature. As explained above, these coefficients are expected to capture the vast majority of the temperature dependence of an EDFA. A simple model can then easily compute EDFA performance at any temperature. Of course, the coefficients shown above are expected to accurately represent the dependence of EDF spectra only for fibers of similar compositions. However, the authors have only observed minor differences for a variety of silica-based, aluminum-codoped EDFs with a wide range of germanium and aluminum levels. This might be expected since the spectrum itself is only slowly dependent on the absolute level of aluminum present. Confirmation of this generalization will be the focus of future work. Even if the data shown here does not generalize to another host, the method certainly does. Hence, at worst case, capturing the temperature dependence of an EDFA in a different host only requires the measurement of parameters at two temperatures. In the simplest case, McCumber's relation can be used to compute the gain coefficient from the absorption coefficient so that only absorption at two temperatures needs to be measured to predict EDFA performance at all temperatures.

In reality, the temperature dependence of the spectrum of an EDFA can often be explored without even running a complete computer model. In particular, many EDFAs operate in such a manner that pump power is varied to set the gain to the desired level. In this case, the fact that average inversion is temperature dependent is irrelevant to the spectrum produced. The pump power must be adequate to achieve the desired gain at all temperatures. Then the spectrum can be computed using (16) and the known temperature dependencies. The average inversion can be determined such that the required gain is achieved at each temperature. The only effect neglected by this approach is spectral hole-burning (SHB). However, assuming that an EDFA is filtered to flatness at the design temperature, SHB is accounted for in the filter. Since the SHB is a relatively small effect, most of the temperature dependence should be captured in a homogeneous treatment.

An example of this sort of approach is illustrated in Fig. 11. In this case, an ideal filter was assumed at 20C to perfectly flatten a 25 dB EDFA between 1528 nm and 1563 nm. The EDFA was assumed to maintain the same constant output power (same average gain) by controlling pump power for all temperatures. The result of Fig. 11 is independent of EDFA design except for the relatively small effect of SHB. Fig. 11 clearly shows that an EDFA cannot be expected to maintain flatness over a broad spectrum over a wide temperature range. The error is greatest on the edge of the spectrum and is not linear. Reducing the temperature by a certain number of degrees has a greater effect than raising the temperature. This is expected from the Boltzmann-like form observed for the emission and absorption coefficients since this form has a smaller derivative the higher the temperature.

The knowledge of the analytical dependence of the gain $g(\lambda, Inv, T)$ in (16) can be used to find optimum parameters for an amplifier. For example, if the amplifier is being designed to maintain gain at a certain wavelength for various temperatures, then one can find optimum wavelength, at which gain is fixed, in such a way that the temperature variation of the gain spectrum is minimal. This can be done by finding derivative $\partial g/\partial T$ for fixed g at certain wavelength (3 dB/m for our example), where temperature dependence of α is taking in the form of (21) and g^* is found via McCumber relation (18). The resulting equation is too complex to provide here, but some results are shown in Fig. 12. The numbers near the plots indicate the wavelength at which gain has been fixed. One can easily judge at what wavelength the gain should be fixed in order to achieve minimum gain variation within the required wavelength range.

VI. Conclusion

We have developed a simple theory to describe the temperature dependence of emission and absorption coefficients for er-

bium-doped fibers. McCumber's relation has been rederived in the view of temperature dependence. The main assumption of the theory is that the temperature changes are due to the dependence of electron distribution over erbium sub levels on fiber temperature. Further simplifications are done to build two numerical models. The actual measurements show that both suggested approximations (21) and (24) work with good accuracy for both signal and pump bands. Each approximation has its own advantages either in precision or in ease of use. In conjunction with McCumber's relation, the approaches described greatly simplify the computer modeling of EDFAs over temperature while providing unique insight into the physical processes involved.

REFERENCES

[1] N. Kagi, A. Oyobe, and K. Nakamura, "Temperature dependence of the gain in erbium-doped fibers," *IEEE J. Lightwave Technol.*, vol. 9, pp. 261–265, 1991.

[2] M. Yamada, M. Shimuzu, M. Horiguchi, and M. Okayasa, "Temperature dependence of signal gain in Er^{3+}-doped optical fiber amplifiers," *IEEE J. Quantum Electron.*, vol. 28, pp. 640–648, 1992.

[3] J. Lee and N. Park, "Temperature dependent distortion of multichannel gain flatness for silica and ZBLAN-based erbium amplifiers," in *Tech. Digest OFC'98*, 1998, Paper WG1, pp. 133–134.

[4] ——, "Reduction of temperature-dependent multichannel gain distortion using a hybryd erbium-doped fiber cascade," *IEEE Photon. Technol. Lett.*, vol. 10, pp. 1168–1170, 1998.

[5] W. T. Silfvast, *Laser Fundamentals*. Cambridge, U.K.: Cambridge Univ. Press, 1996, pp. 204–205.

[6] C. Giles and E. Desurvire, "Modeling erbium-doped fiber amplifiers," *J. Lightwave Technol.*, vol. 9, p. 271, 1991.

[7] W. Miniscalco and R. Quimby, "General procedure for the analysis of Er3+ cross sections," *Opt. Lett.*, vol. 16, pp. 258–260, 1991.

[8] D. McCumber, "Theory of phononterminated optical masers," *Phys. Rev.*, vol. 134, pp. A299–A306, Apr. 1964.

[9] ——, "Theory of vibrational structure in optical spectra of impurities in solids. II. Multiplets," *J. Math. Phys.*, vol. 5, pp. 508–521, 1964.

Maxim Bolshtyansky, photograph and biography not available at the time of publication.

Paul Wysocki, photograph and biography not available at the time of publication.

Nicholas Conti, photograph and biography not available at the time of publication.